WIND ENERGY
Wind Energ. 2012; **15**:645–659
Published online 20 September 2011 in Wiley Online Library (wileyonlinelibrary.com). DOI: 10.1002/we.498

RESEARCH ARTICLE

Validation of a double fed induction generator wind turbine model and wind farm verification following the Spanish grid code

Francisco Jiménez[1], Emilio Gómez-Lázaro[2], Juan Alvaro Fuentes[3], Angel Molina-García[3] and Antonio Vigueras-Rodríguez[4]

[1] Gamesa Innovation & Technology, Pamplona (Navarra), Spain
[2] Renewable Energy Research Institute and DIEEAC/EDII-AB, Castilla-La Mancha University, Albacete, Spain
[3] Department of Electrical Engineering, Technical University of Cartagena, Cartagena (Murcia), Spain
[4] Renewable Energy Research Institute and DIEEAC/EDII-AB, PCYTA—Castilla-La Mancha University, Albacete (Castilla-La Mancha), Spain

ABSTRACT

Wind turbine manufacturers are required by transmission system operators for fault ride-through capability as the penetration of wind energy in the electrical systems grows. For this reason, testing and modeling of wind turbines and wind farms are required by the national grid codes to verify the fulfillment of this capability.

Therefore, wind turbine models are required to simulate the evolution of voltage, current, reactive and active power during faults. The simulation results obtained from these wind turbine models are used for verification, validation and certification against the real wind turbines measurement results, although evolution of electrical variables during the fault and its clearance is not easy to fulfill.

The purpose of this paper is to show the different stages involved in the fulfillment of the procedure of operation for fault ride-through capability of the Spanish national grid code (PO 12.3) and the 'procedure for verification, validation and certification of the requirements of the PO 12.3 on the response of wind farms in the event of voltage dips'. The process has been applied to a wind farm composed of Gamesa G52 wind turbines, and the results obtained are presented. Copyright © 2011 John Wiley & Sons, Ltd.

KEYWORDS

fault ride-through capability (FRT); voltage dip; wind turbine modeling; simulation; validation

Correspondence

Emilio Gómez-Lázaro, Renewable Energy Research Institute and DIEEAC/EDII-AB, Castilla-La Mancha University, Albacete, Spain.
E-mail: emilio.gomez@uclm.es

Received 10 June 2010; Revised 28 March 2011; Accepted 28 May 2011

1. INTRODUCTION

Spain defined a procedure for measuring and evaluating the response of wind turbines and wind farms submitted to voltage dips[1]—procedure for verification, validation and certification of the requirements of the PO 12.3 on the response of wind farms in the event of voltage dips (PVVC). The result of following this procedure leads to the certification of its conformity with the response requirements specified in the Spanish grid code.[2] Some aspects related to that grid code are explained with some detail in Gómez-Lázaro *et al.*[3]

Grid codes are usually different among countries, even in the European Union. In this way, some researchers have performed grid code comparisons between some of them[4] and even studies about unified or standardized requirements.[5–7] Moreover, the importance of standardizing the technical compatibility requirements for wind generators has been highlighted by the Union for Coordination of Transmission of Electricity (UCTE), now part of the European Network for Transmission System Operators for Electricity.[8–10]

The importance of the standardization is about not only the technical requirements but also the electrical simulation models. Working group for IEC 61400-27 standard[11] is studying electrical simulation models for power systems and grid

stability analysis. Its purpose is to define standard dynamic simulation models for wind turbines and wind power plants, which are intended for used in power system and grid stability analyses, and it should be applicable for dynamic simulations of power system events such as short circuits (low-voltage ride through), loss of generation or loads, and system separation.

This paper follows the different stages of the Spanish grid code and PVVC. In Section 2, the PVVC is summarized, whereas Section 3 is dedicated to the details of the voltage dip test generator. Finally, Section 4 presents the different results obtained along the verification process of a wind farm model using the validated wind turbine model.

2. SPANISH PROCEDURE FOR VERIFICATION, VALIDATION AND CERTIFICATION

The certification process of PVVC comprises the following verifications:

- Verification that the wind farms do not disconnect as a consequence of voltage dips in the point of common coupling (PCC) associated with correctly cleared short circuits according to the voltage time curve specified in the grid code.[2]
- Verification that the power and energy consumption (active and reactive) in the PCC, for balanced and unbalanced faults, is less than or equal to the levels marked in the grid code.[2]

Figure 1 shows the verifying process flow diagram, which may be completed by executing two optional branches: the general verification process (marked with solid lines) and the particular verification process (-marked with dotted lines).

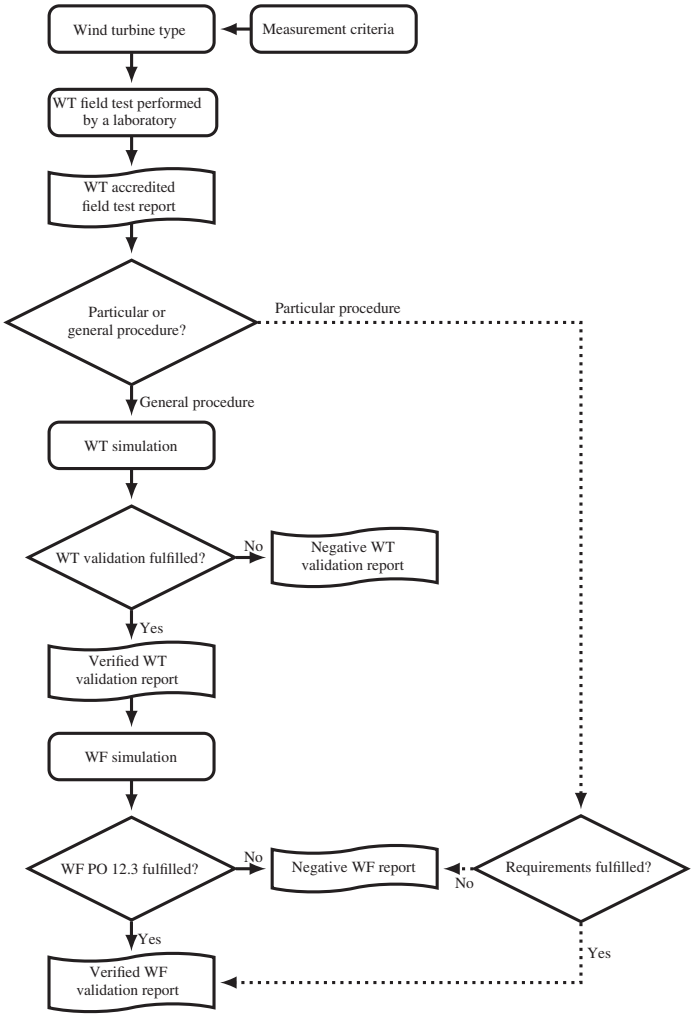

Figure 1. Flow chart of the stages of the verification process.

Wind Energ. 2012; **15**:645–659 © 2011 John Wiley & Sons, Ltd.
DOI: 10.1002/we

Different PVVC editions have appeared taking into account the contributions of actors with presence in the Spanish wind energy industry, including the authors of this paper, to overcome the difficulties that appeared in its initial implementation.

2.1. General verification process

The general process consists of verifying the PCC requirements of a wind farm stated in the grid code. As testing a wind farm is too complex and expensive, the approach followed by the PVVC has been the validation of single wind turbines and the simulation of the behavior of the wind farm by using the validated models of its wind turbines. The full process is divided in three stages:

- Wind turbine test.
- Wind turbine model validation.
- Wind farm simulation.

2.1.1. Wind turbine field test

The wind turbine must be tested in the field with voltage dips fixed in the PVVC. The PVVC also recommends to perform the tests on a voltage dip generator based on an inductive divider (Figure 2) and explains the calculation procedure for reactances X_1, X_2 and X_3.

According to the PVVC, wind turbines should be tested in the field with two different types of voltage dips and two different operation points.

The voltage dip tests must be a three-phase and two-phase isolated voltage dip, and they must be carried out using a voltage dip generator.

The operation points are function of the rated active power of the wind turbine P_n, and they must be inside the following ranges: a full load range ($\geq$80% P_n) and a partial load range (10%–30% P_n). Table I reflects the four categories of allowed tests.

The reason for considering two different operation points in the PVVC is due to the slightly different behavior of the wind turbine depending on the working point. For example, DFIG wind turbines commonly use two different control strategies depending on the wind speed profiles: one for low wind speed and the other for high-speed wind where the wind turbine is working with rated rotor speed.

As the result of the voltage dip test, voltages and currents of the three phases are captured in the so-called measurement point. This point could be different from the fault point in case the measurement is performed in the low-voltage side or the high-voltage side of the wind turbine transformer.

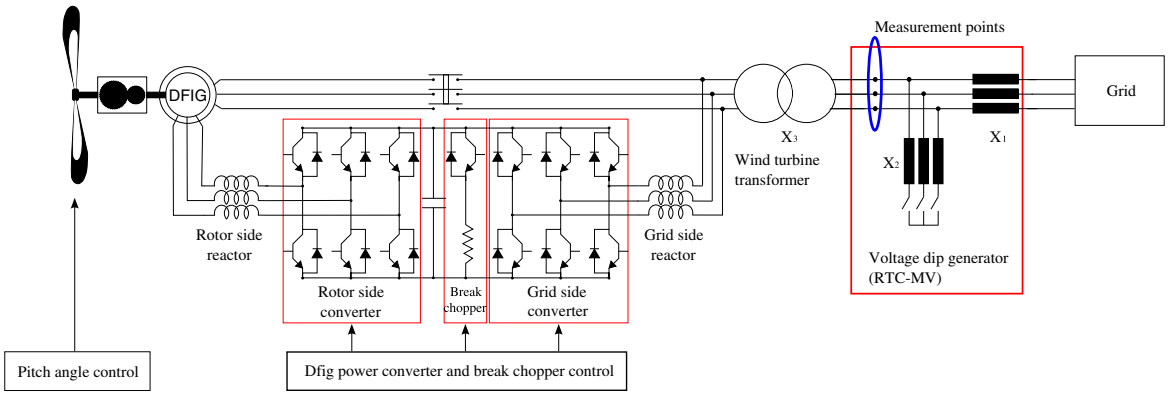

Figure 2. Double fed induction generator (DFIG) wind turbine scheme with the voltage dip generator equipment (RTC–MV).

Table I. Test categories to be performed taking into account the operation point and the voltage dip type according to PVVC.

Category	Load	Active power	Power factor	Voltage dip type
1	Partial load	10%–30% P_n	0.90 ind.–0.95 cap.	Three phase
2	Full load	$\geq$ 80% P_n	0.90 ind.–0.95 cap.	Three phase
3	Partial load	10%–30% P_n	0.90 ind.–0.95 cap.	Two-phase isolated
4	Full load	$\geq$ 80% P_n	0.90 ind.–0.95 cap.	Two-phase isolated

Table II. Voltage dip properties in the no load test according to the PVVC.

Type of dip	U_{res}	U_{tol}	T_{dip} (ms)	T_{tol} (ms)
Three phase	$\leq (20\% + U_{tol})$	+3%	$\geq (500 - T_{tol})$	50
Two-phase isolated	$\leq (60\% + U_{tol})$	+10%	$\geq (500 - T_{tol})$	50

Wind turbine tests are accepted as valid when the following requirements are met:

- Active and reactive power recorded before the voltage dip test must be within the intervals defined in Table I.
- Continuity of supply. The wind turbine is not disconnected during the application of the voltage dip in three consecutive tests in the same category.
- The residual voltage, U_{res}, must be lower than that specified in Table II with the wind turbine disconnected, taking into account the voltage tolerance, U_{tol}. Moreover, the voltage dip duration (T_{dip}) and the time tolerance (T_{tol}) must be taken into account.

2.1.2. Wind turbine model validation

The wind turbine simulation model must be validated with the measurements recorded and accredited in the field tests according to Tables I and II.

Wind turbine model validation requires the following steps:

- Using the wind turbine field tests, the fundamental harmonic of voltage and current root mean square (RMS) values are determined, with active and reactive power being computed too.
- The same instantaneous variables as those recorded in the test are simulated using the wind turbine model. The simulation must be carried out with a time stepping equal or less than the equivalent sampling frequency in the field tests. The same procedure is used for obtaining the RMS values of fundamental harmonics of voltages and currents, together with the active and reactive power.

The simulation of the wind turbine is carried out using a dependent voltage source as model of the electrical grid and the test bench, with the voltage profiles imposed by the recorded ones in the field test.

The wind turbine model is validated when for 85% of the active and reactive data series, the difference between simulated (P_{sim}, Q_{sim}) and field test (P_{mea}, Q_{mea}) values do not exceed 10% with respect to the rated data (P_{rated}, Q_{rated}), where $Q_{rated} = P_{rated}$.[1] For this comparison, a data window with 1 s duration is defined. The start of the data window is 100 ms before the voltage dip.

$$\Delta P(\%) = \frac{P_{mea} - P_{sim}}{P_{rated}} \cdot 100 \leq 10\% \tag{1}$$

$$\Delta Q(\%) = \frac{Q_{mea} - Q_{sim}}{Q_{rated}} \cdot 100 \leq 10\% \tag{2}$$

2.1.3. Wind farm simulation

The validated simulation models of all dynamic elements of the wind farm, including wind turbines and/or FACTS, must be integrated into a wind farm simulation model. The final process is the fulfillment of the requirements imposed by the Spanish grid code. A verified wind farm report is obtained after evaluating the response of the entire wind farm model.

2.2. Particular verification process

The particular verification process was developed to simplify the general process. In the particular procedure, the wind farm verification can be obtained by testing the dynamic elements of the wind farm, without carrying out computer simulations. In this case, both the conditions in the field test and the validation criteria are harsher than the ones in the grid code and in the general verification process. Therefore, if the wind turbine is validated, it is considered that the wind farm will always be validated without necessity of a simulation.

3. FIELD TESTS

Gamesa initial designs for the voltage dip generator were based on wind turbine components, using wind turbine transformers as series and parallel impedances (X_1, X_2 and X_3; Figure 2). Parallel impedance was composed of three transformers.

Wind Energ. 2012; **15**:645–659 © 2011 John Wiley & Sons, Ltd.
DOI: 10.1002/we

This test bench was used from 2004 to 2006 in the first voltage dip tests, and its results were used in the draft proposal of PVVC. However, technical limitations of this configuration led to the development of two equipments between the end of 2005 and mid-2006: the 'ride-through container–low voltage' (RTC–LV) and the 'ride-through container–medium voltage' (RTC–MV).[12] For this study, the RTC–MV is employed.

Test equipment based on an inductive divider are flexible enough to obtain fault effects in wind turbines, whose required characteristics are given by national grid codes or even specified in international standards as the second edition of the IEC 61400-21.[8]

The RTC–MV unit was designed to generate the required faults in the verification process as this unit allows programming the value of the voltage dip in steps of around 20%, with the disturbance duration range from 0.05 to 3 s. Furthermore, the voltage recovery shape can be modified to reproduce response times near to real cases as are defined in some grid codes too.[2] The equipment is composed of three reactors (Figure 2). The total impedance of the series reactor X_1 limits the short-circuit current during the fault, and its value is calculated on the basis of the grid short circuit. The parallel reactor X_2 determines the residual voltage, and it is being composed of a set of reactors in series. The series reactor X_3 simulates the wind turbine transformer. The RTC–MV design satisfies the X_3 reactor requirements because X_3 is, in fact, the wind turbine transformer.

Reactors X_1 and X_3 could be made of single reactors or a combination of reactors and transformers according to the PVVC.

The X_1 reactance is calculated in a way that the short-circuit power in the test point is greater than or equal to five times the registered power of the wind turbine:

$$X_1 \leq \frac{U_n^2}{5 \cdot S_n^{WT}} - Z_{cc} \tag{3}$$

where $\bar{Z}_{cc}$ is the short-circuit impedance of the grid, U_n the rated voltage and S_n^{WT} the wind turbine rated power.

X_2 reactance is calculated such that for each of the four test categories—described in Table I and with voltage dip characteristics shown in Table II—the minimum RMS voltage, U_{res}, registered during the no load test of the fault phases is less than 90% of the rated voltage. In this way, it could be obtained from the following expression:

$$U_{\text{res}} = U_n \cdot \left| \frac{jX_2}{\bar{Z}_{cc} + jX_1 + jX_2} \right| \tag{4}$$

Finally, X_3 reactance has to comply with the following conditions depending on whether the wind generator has or has not a step-up transformer:

- Without step-up transformer, $X_3 = 0$.
- With a step-up transformer, there are two cases:
  - X_3 will take the value of the short-circuit impedance of the step-up transformer.
  - X_3 will take the value of the short-circuit impedance of the step-up transformer in normalized value with a tolerance of $\pm 20\%$.

The RTC–MV design satisfies the X_3 reactor requirements because X_3 is, in fact, the wind turbine transformer.

4. RESULTS

A real wind turbine (Gamesa G52; see Table III) modeled with the PSCAD/EMTDC software package (Manitoba HVDC Research Centre, Winnipeg, Manitoba, Canada) using a time step of 10.024 μs and taking into account the real mechanical, electrical and electronic subsystems—design, parameters and algorithms—such as the power converter, IGBTs control,[13–15] is going to be submitted to the validation process. The G52 power converter (DAC, dip active converter) was designed to fulfill the Spanish grid code.[16] Previously, the mechanical model subsystem was compared with a detailed model using BLADED software package (Garrad Hassan and Partners Limited, Silverthorne Lane, Bristol, UK), and the electrical subsystem was compared with the test bench results.

4.1. Voltage dip modeling

Wind turbine model response to voltage dips is obviously affected by not only the precision of the model itself but also their inputs—voltage waveforms. Therefore, accuracy of voltage waveforms, specifically during the beginning of the voltage dip and the fault clearance, is needed. To obtain the best fit between the simulated results and the test ones, authors proposed that voltage waveforms were to be modeled as voltage-dependent sources fed by the measured voltage waveforms from the tests. In the fourth and previous PVVC editions, a physical model of the test bench and the grid was required in the validation process, but with the fifth and following editions, the voltage-dependent source is required (Table IV).

Table III. Gamesa G52 main specifications.

Power	
Rated power	850 kW
Cut-in wind speed	4 m s^{-1}
Cut-out wind speed	25 m s^{-1}
Rated wind speed	15 m s^{-1}
Rotor	
Rotor diameter	52 m
Rotor speed	14.6–30.8 rpm
Blade number	3
Blade length	25.3 m
Hub mass with blades	10,000 kg
Blade mass	1900 kg
Top head mass	33,000 kg
Tower	
Tower height	65 m
Tower mass	79,000 kg
Gearbox	
Gearbox stages	3
Gearbox type	One planetary and two helical stages
Gearbox ratio	1 : 61.74 (50 Hz)
Generator	
Generator type	Asynchronous, double fed induction
Speed range	900–1900 rpm
Generator voltage	690 V
Control system	
Wind turbine type	Variable speed
Power limitation	Pitch

Table IV. Evolution of requirements collected over different PVVC editions.

PVVC edition	1, 2	3, 4	5, 6, 7
Release date	January 2007	November 2007, March 2008	June 2009, July 2009, February 2010
Partial load test, P	10%–30% P_n	10%–30% P_n	10%–30% P_n
Partial load test, $\cos\varphi$	0.95 ind.–0.95 cap.	0.90 ind.–0.95 cap.	0.90 ind.–0.95 cap.
Full load test, P	$\geq$80% P_n	$\geq$80% P_n	$\geq$80% P_n
Full load test, $\cos\varphi$	0.95 ind.–0.95 cap.	0.90 ind.–0.95 cap.	0.90 ind.–0.95 cap.
Reference X_{ref}*	Measured value	Measured value	Rated value
Active power	Yes	Yes	Yes
Reactive power	Yes	Yes	Yes
RMS fundamental phase voltage	Yes	Yes	No
RMS fundamental phase current	Yes	Yes	No
Comparison window, Figure 6	$[T_2, T_4]$ *or* $[T_2, T_3 + 150$ ms$]$	$[T_2, T_4]$ *or* $[T_2, T_3 + 150$ ms$]$	$[T_1 - 100$ ms, $T_1 + 900$ ms$]$
Voltage dip modeling	Fault equipment model	Fault equipment model	Voltage source

* $\Delta X(\%) = (X_{mea} - X_{sim})/X_{ref}$.

Figure 3 shows the comparison between the phase voltage waveforms in the wind turbine medium voltage terminals (Figure 2), at the beginning and during the clearance of the fault, between the measured voltage dip and the simulated one, using in the simulation the proposed physical model of the test bench of the fourth PVVC edition.

Figure 3(a)–(c) shows almost the same evolution of the three-phase voltages during the beginning of the fault. However, during the clearance of the voltage dip, differences are seen in all phases and especially in R phase (Figure 3(d)). This surge is a common effect in this test equipment, being even more accused in the low-voltage ones.[14] Therefore, the circuit breaker clearing the fault should model in some detail the non-simultaneous breaking of the phase currents and the arc,[17] if an adequate precision is needed as it is required in this application.

These voltage waveforms affect the transformer by causing an inrush current, provoking differences in voltages and reactive power.

Wind Energ. 2012; **15**:645–659 © 2011 John Wiley & Sons, Ltd.
DOI: 10.1002/we

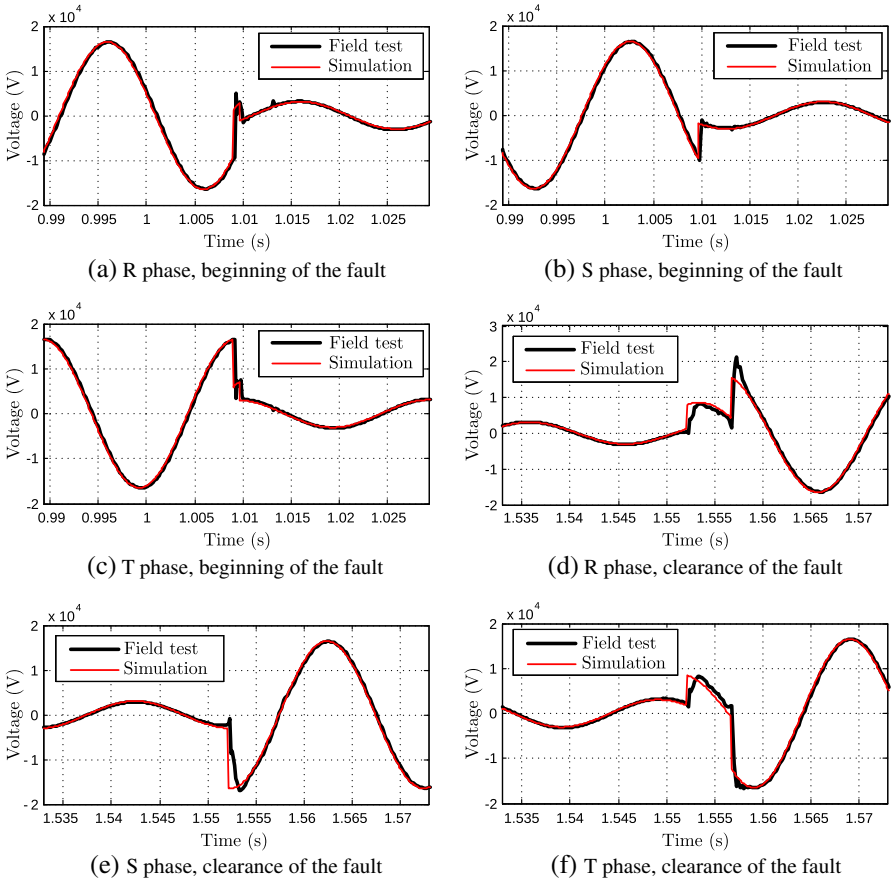

Figure 3. Measured and simulated voltage waveforms during the voltage dip.

4.2. Wind turbine modeling

Fault ride-through capability requirements define the electrical behavior, usually in terms of active power and reactive power, together with reactive currents, during the voltage dip and the voltage recovery period after the clearance of the fault. Therefore, the validation criteria must address the accuracy requirements between test and simulation for that magnitudes. The comparison interval—comparison window—should be between the start of the voltage dip and the time subsequent to the recovery of the undisturbed state. Table IV shows the comparison windows considered in all the PVVC editions.

For the validation process required by the grid code of the wind turbine, its model should represent the fault ride-through capability, and therefore, the protections of the real wind turbine must be considered. In this way, a good correlation between test and simulation results is needed, especially in the variables capable of firing the alarms. In some cases, the response of active and reactive power is affected by rapid changes in the instantaneous values of current or voltages due to the power converter controls. So in case of DFIG wind turbines with break chopper, instantaneous values of rotor currents will affect rotor converter controller, and direct current (DC) bus voltages can fire the break chopper, changing substantially the response in terms of active and reactive power. The break chopper protection method burns the excess of active power coming from the rotor of the generator to the DC link (Figure 2). Therefore, although the rotor current and the DC bus voltage are not directly variables to compare, good accuracy in them is required because of their influence in the evolution of active and reactive power.

4.3. Wind turbine validation

Wind turbine is submitted to a three-phase voltage dip with a retained voltage of 20% (19.66%, 17.75% and 19.91% for R, S and T phases, respectively) and a duration of 0.5705 s, being a valid test from the PVVC point of view (Table II). In Figure 4, the phase voltage waveforms at the point of interconnection are shown, whereas Figure 5 shows the phase

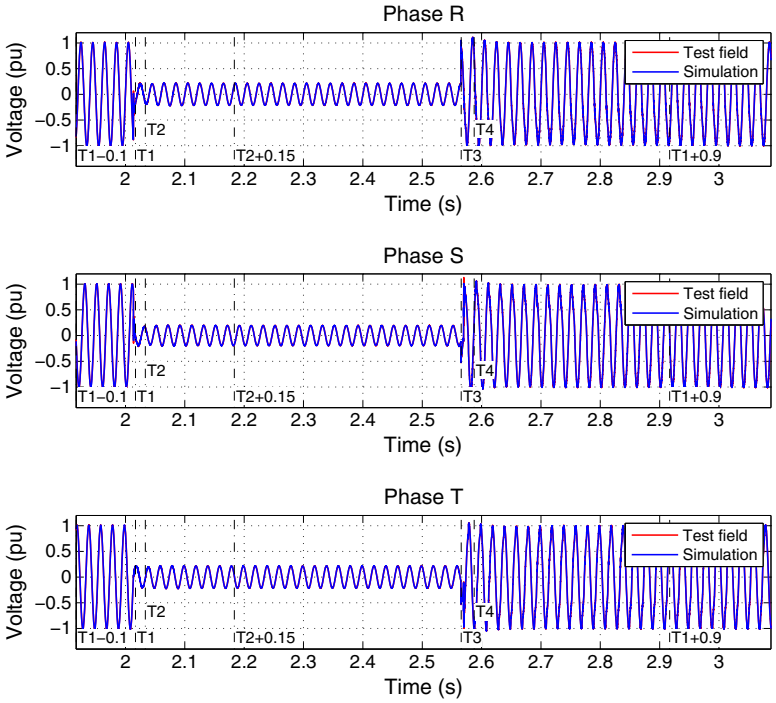

Figure 4. Voltage waveforms at the point of interconnection.

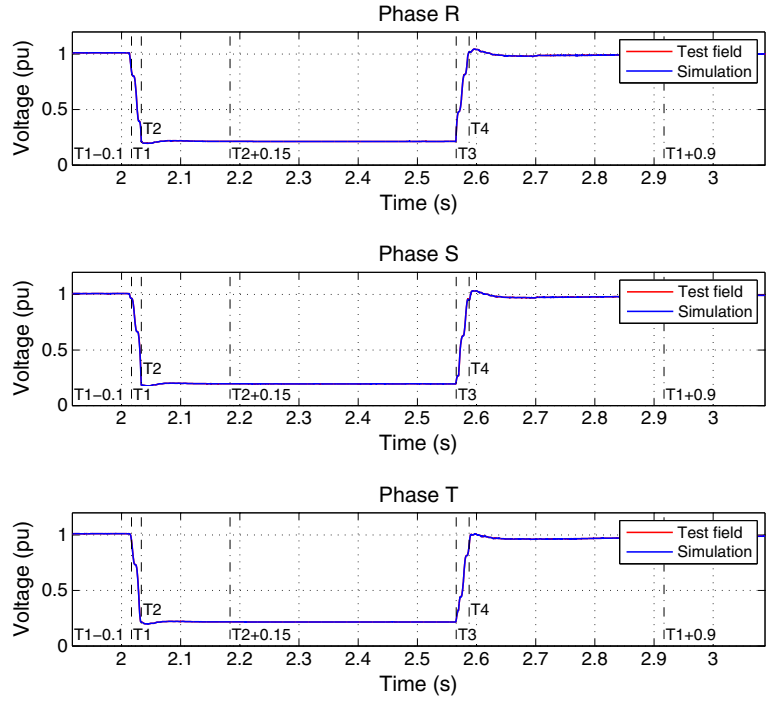

Figure 5. RMS voltage at the point of interconnection.

RMS voltages. During the beginning and the clearance of the fault, some surges appear in the voltage waveforms (see Section 4.1), small differences being observed even in the RMS values. Figures 4 and 5 show the zones defined in the PVVC and the Spanish grid code bounded by T_1, T_2, T_3 and T_4 (Figure 6).

Wind Energ. 2012; **15**:645–659 © 2011 John Wiley & Sons, Ltd.
DOI: 10.1002/we

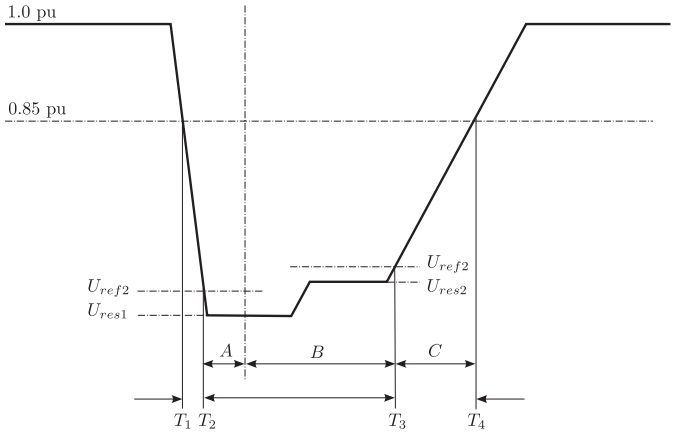

Figure 6. Classification of zones during the voltage dip.

The PVVC and the Spanish grid code defines different zones in which the wind farm response could be different (Figure 6). T_1, T_2, T_3 and T_4 are defined as follows:

- T_1, start of dip. It is the instant in which the voltage $U_{\text{ef}(1/4)}$ of one of the phases falls below the dip threshold of 0.85 pu.
- T_4, end of dip. It is the instant in which the voltage $U_{\text{ef}(1/4)}$ in all of the channels measured is equal to or greater than the dip threshold.
- T_2 and T_3, start and end of the bottom of the dip. They are defined by the instants determined from the voltage values $U_{\text{ef}(1/4)}$ measured.

Figure 7 shows the evolution of current waveforms. Some differences appear at the beginning of the voltage dip and at the beginning of the clearance of the fault, the field test and simulation results being quite similar, even the bigger peaks

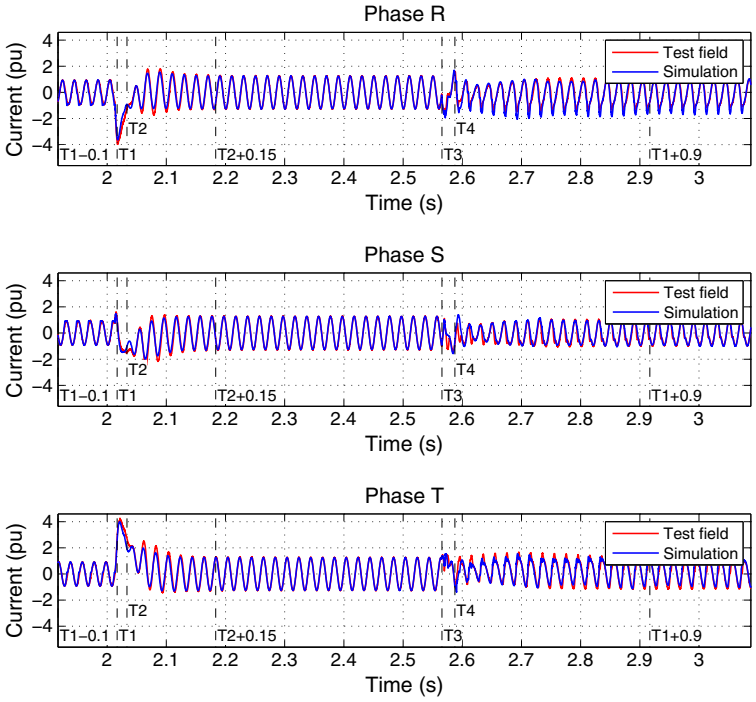

Figure 7. Current waveforms at the point of interconnection.

obtained between T_1 and T_2 marks. Between T_2 and T_2+150 ms (area A defined in PVVC; Figure 6), unbalanced currents appear in this interval, being progressively reduced and gaining at the same time their balanced state. Between T_3 and T_4, currents suffer unbalanced states as well, being reduced from T_4, although measured and computed results show some differences (mainly in peak values).

Figure 8 shows the RMS currents. Comments are obviously similar to the ones stated before. So, in the R phase (Figure 8(a)), peaks are obtained between T_1 and T_2 and between T_2 and $T_2 + 150$ ms, with some differences in results from test and simulation. Between $T_2 + 150$ ms and T_3, the two curves are almost identical (as in the other two-phase currents). From T_3 and T_4, some differences are observed between them. Figure 8(b) shows a better agreement in the S phase current, except between T_2 and $T_2 + 150$ ms. T phase current (Figure 8(c)) shows a good fit between measured and computed results, with some differences.

The active and reactive power evolution are shown in Figure 9, which are obtained from the positive sequence component of voltages and currents. Active power (Figure 9(a)), presents an almost perfect fit between the field test and simulation results, showing some differences from T_4 and around 2.8 s. In that figure, the intervals marked in black are those whose difference between the simulated and field test results do not exceed 10% with respect to the rated wind turbine (equation (1)), whereas those who exceed the 10% limit are marked in pink.

Figure 9(b) presents the reactive power evolution, showing a good fit between the field test and simulation results. Again, the same color code is used for the 10% limit (equation (2)). There are four intervals in which the threshold value are exceeded. The first one is between T_1 and T_2, being the second one bigger, around T_4, and the remaining around 2.7 and 2.9 s.

The voltage dip influence over the DFIG rotor speed is presented in Figure 10, the field test and simulated results being quite similar, and showing the over speed evolution and the slower transients in the wind turbine mechanical subsystem.

Table V summarizes the results obtained for active and reactive power of the wind turbine according to the PVVC validation process. The wind turbine model is validated when for 85% of the active and reactive data series, the difference between simulated (P_{sim}, Q_{sim}) and field test (P_{mea}, Q_{mea}) values do not exceed 0.1 pu. As the results obtained are 91% and 90%, respectively, the conclusion is that the wind turbine model validation requirements is fulfilled.

One final comment could be made about the currents (Table V), which are under 85% in all cases (59%, 82%, 74%). This is because currents are much more difficult to fit than active and reactive power because of the aggregation process involved in their definitions. Up to the fourth PVVC edition, RMS values of fundamental harmonic voltages and currents in each phase were used as requirements in the validation process (Table IV), but authors suggested that current comparisons should be excluded from the PVVC because transmission system operators consider active and reactive power evolution the key magnitudes to take into account during voltage dips.

4.4. Wind farm simulation

The final part of the simulation procedure consists of the evaluation of the wind farm response to voltage dips. The wind farm model has to take into account the equivalent electrical network and the wind turbines and the internal topology of the wind farm or an aggregation of the wind turbines, in case the wind farm is composed of wind turbines of the same model. A fault must be applied to the grid connection point for the four test categories (Table I). Figure 11 shows the single-phase equivalent diagram considered for the wind farm model, where it can be seen the aggregated model of the wind farm used, and for the equivalent electrical grid model that represents the Spanish electrical system. This latter grid is composed of different nodes that models the dynamic behavior of UCTE (UCTE node), the dynamics of the closest electrical grid (RED node) and the grid connection point (GCP node) of the wind farm. The three nodes are connected through impedances of selected values that allows to reproduce the typical voltage profile of the Spanish electrical system voltage dips.[1]

Once the simulations have been carried out, the fulfillment of the following requirements must be proven for each test category:

- Continuity of supply. The wind farm must withstand the specified dips without disconnection.
- Voltage and current levels at the wind turbine terminals. The residual simulated voltage in the test measuring point is equal or higher than the measured in the field test, with a tolerance of 2%, and the maximum simulated currents in the A and C zones defined in Figure 6 are lower than the measured ones in the test measuring point.
- Active and reactive power and reactive current must comply with exchange limits defined by the Spanish grid code.[2]

where $U_{\text{ef(1/4)}}$ is defined by the value of the effective voltage measured in a period and updated every quarter of a cycle.[18]

Tables VI and VII show the results obtained with the simulation of the wind farm under the Spanish grid code requirements with three-phase and two-phase voltage dips. These requirements are classified by the zones (A, B and C) defined in Figure 6, being detailed in Gómez-Lázaro *et al.*[3] All the requirements are fulfilled by the wind farm simulation.

Wind Energ. 2012; **15**:645–659 © 2011 John Wiley & Sons, Ltd.
DOI: 10.1002/we

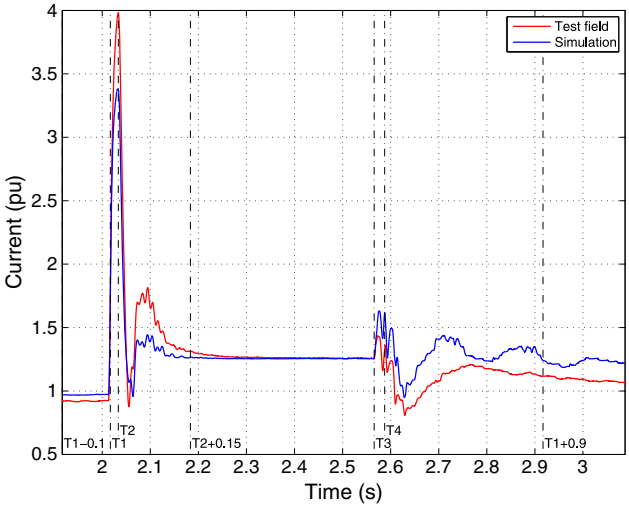

(a) R phase

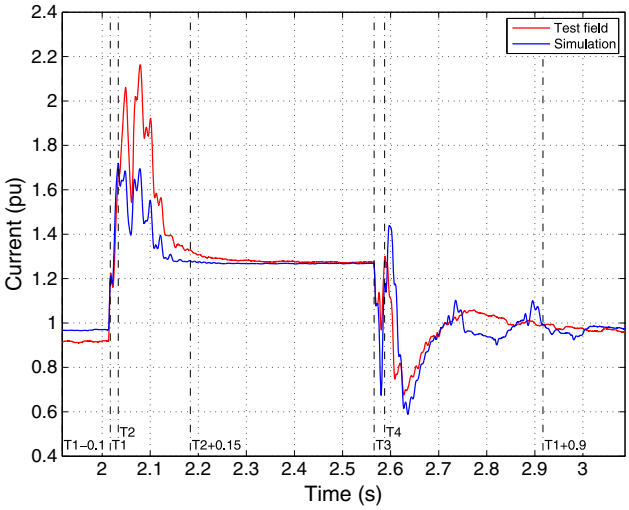

(b) S phase

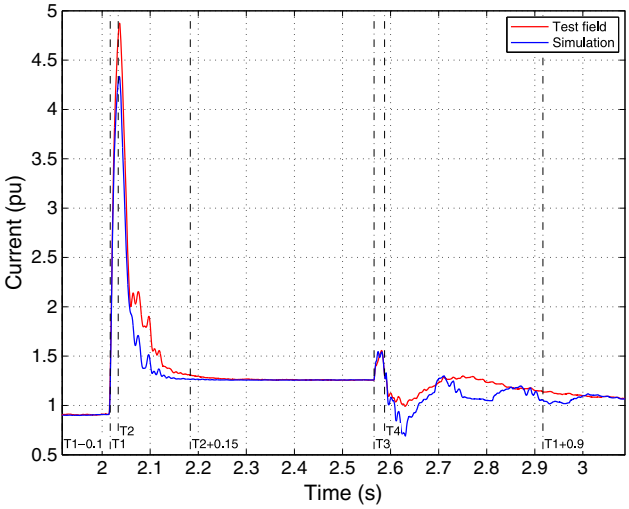

(c) T phase

Figure 8. RMS current at the point of interconnection.

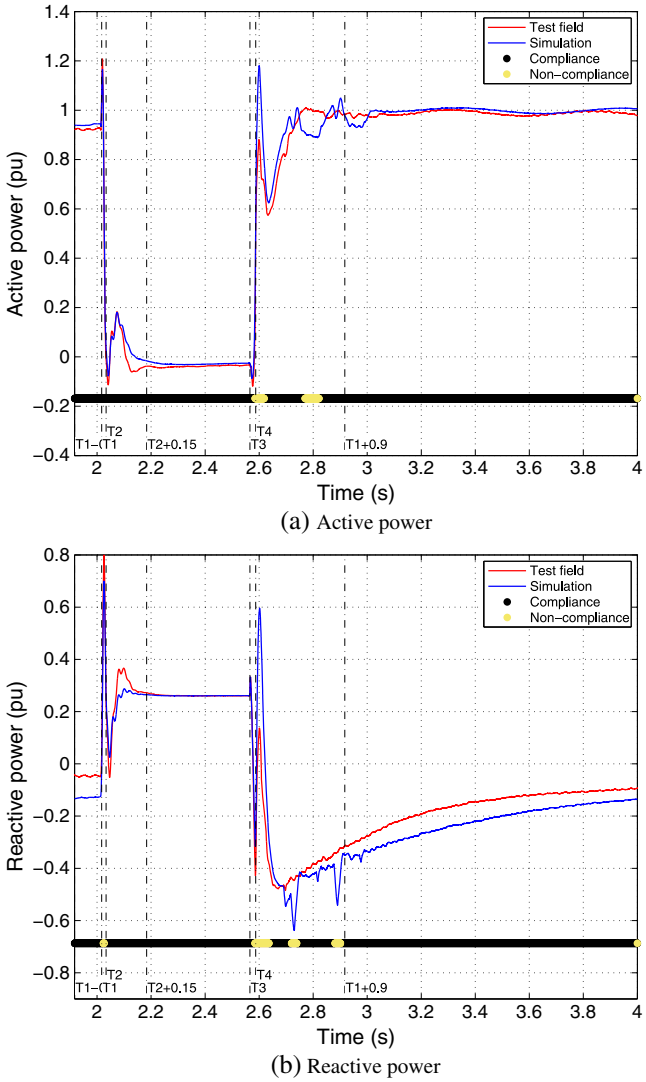

(a) Active power

(b) Reactive power

Figure 9. Active and reactive power at the point of interconnection.

In addition, wind farm complies with the continuity of supply requirement since wind farm has not trip in any case of the simulation. Finally, Tables VIII and IX show the evaluation of voltage and current levels at the wind turbine terminals. For this purpose, the maximum current of all phases in the wind turbine terminals in simulation has been compared with those in the test results. For voltage, the residual voltage in phase-to-neutral basis from test has been compared with the phase-to-phase voltage from simulation because the delta-star wind farm substation transformer changes voltage phasors from phase-to-neutral to phase-to-phase.

5. CONCLUSIONS

The general verification process of the Spanish PVVC has been followed for a wind farm composed of Gamesa G52 wind turbines, which has been verified to comply with the requirement imposed by the Spanish grid code. Along the process, the wind turbine model has been validated, fulfilling the requirements of the PVVC.

The results have shown good agreement between computed and measured values defined in the Spanish grid code. The key aspects of the verification, validation and certification processes involved in the Spanish grid code are highlighted, and even the modification of certain requirements in the different procedure editions are justified.

Wind Energ. 2012; **15**:645–659 © 2011 John Wiley & Sons, Ltd.
DOI: 10.1002/we

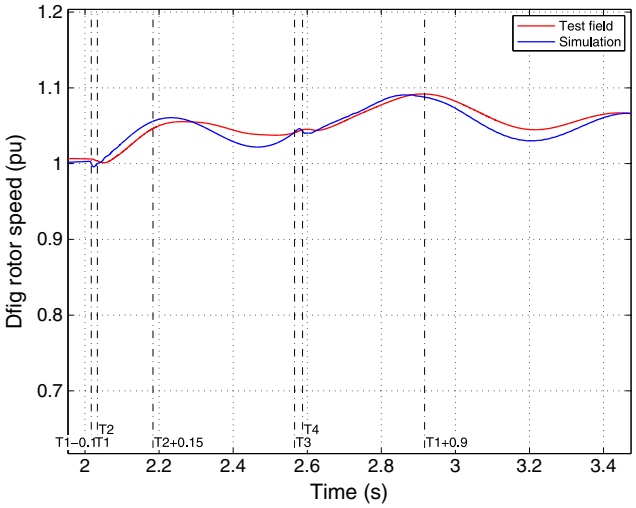

Figure 10. DFIG rotor speed.

Table V. PVVC results.

Magnitude	PVVC maximum error (pu)	PVVC points (%), 0.1 pu	Points (%), 0.1 pu	Fulfillment
P	0.10	0.85	0.91	Yes
Q	0.10	0.85	0.90	Yes
I_r[a]	0.10	0.85	0.59	No
I_s[a]	0.10	0.85	0.82	No
I_t[a]	0.10	0.85	0.74	No

[a]Not in PVVC.

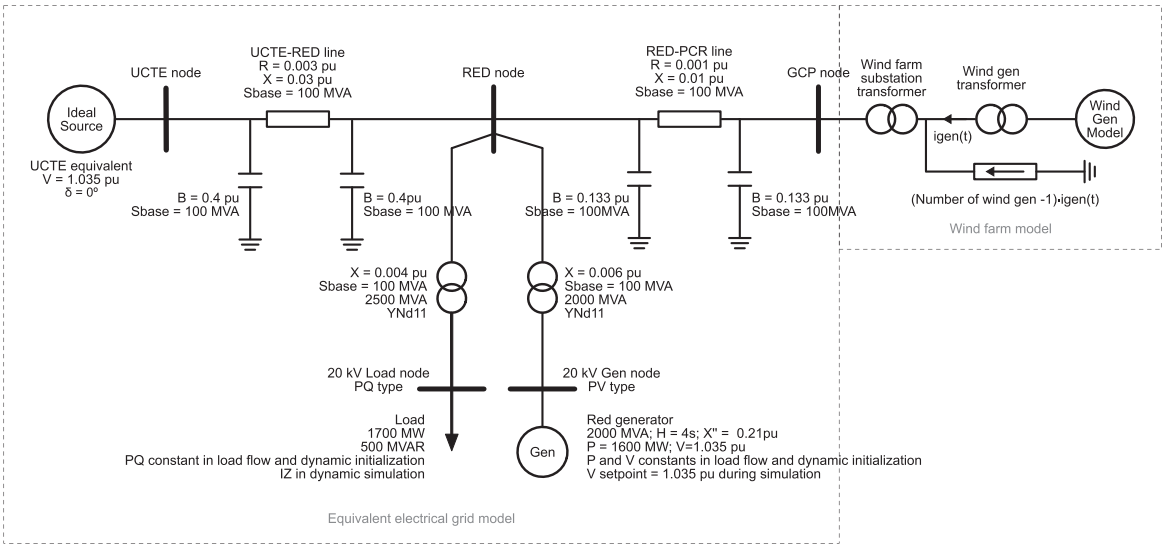

Figure 11. Equivalent electrical grid and wind turbine models (single-line scheme).

ACKNOWLEDGEMENTS

The authors would like to thank GAMESA for the technical and financial support. The financial support provided by 'Junta de Comunidades de Castilla-La Mancha' (PEII10-0171-1803) and 'Ministerio de Ciencia y Innovación' (ENE2009-13106) is gratefully acknowledged.

Table VI. PO 12.3 results in zones *A, B* and *C* for three-phase voltage dips.

Magnitude	PO 12.3	Full load		Partial load	
	(pu)	(pu)	Fulfillment	(pu)	Fulfillment
Zone A: reactive power consumption	≤ -0.600 (20 ms)	0.060	Yes	0.043	Yes
Zone B: active power consumption	≤ -0.100 (20 ms)	−0.042	Yes	−0.042	Yes
Zone B: reactive current $I_{reactive}/I_{total}$	≥ 0.900	0.993	Yes	0.991	Yes
Zone C: reactive energy consumption	$\leq 60\% P_{rated} \cdot 150$ ms	0.030	Yes	0.069	Yes
Zone C: reactive current $I_{reactive}$	≤ -1.500 (20 ms)	0.108	Yes	0.247	Yes

Table VII. PO 12.3 results in zones *A, B* and *C* for two-phase voltage dips.

Magnitude	PO 12.3	Full load		Partial load	
	(pu)	(pu)	Fulfillment	(pu)	Fulfillment
Zone B: reactive energy consumption	$\leq 40\% P_{rated} \cdot 100$ ms	0.041	Yes	0.085	Yes
Zone B: reactive power consumption	≤ -0.400 (20 ms)	0.106	Yes	0.238	Yes
Zone B: active energy consumption	$\leq 45\% P_{rated} \cdot 100$ ms	0.270	Yes	0.087	Yes
Zone B: active power consumption	≤ -0.300 (20 ms)	0.783	Yes	0.255	Yes

Table VIII. Voltage and current comparisons in the wind turbine terminals for three-phase voltage dips.

Magnitude	Full load			Partial load		
	Test	simulation	Fulfillment	Test	simulation	Fulfillment
Zone A: current (A)	119.596	81.360	Yes	83.744	77.672	Yes
Zone C: current (A)	38.194	32.003	Yes	36.151	32.185	Yes
Residual voltage (pu)	0.177	0.311	Yes	0.184	0.310	Yes

Table IX. Voltage and current comparisons in the wind turbine terminals for two-phase voltage dips.

Magnitude	Full load			Partial load		
	Test	simulation	Fulfillment	Test	simulation	Fulfillment
Zone A: current (A)	74.655	53.848	Yes	53.922	53.437	Yes
Zone C: current (A)	63.419	43.968	Yes	45.780	31.464	Yes
Residual voltage (pu)	0.619	0.631	Yes	0.621	0.649	Yes

REFERENCES

1. *Procedure for verification validation and certification of the requirements of the PO 12.3 on the response of wind farms in the event of voltage dips*, 7th ed. Spanish Wind Energy Association, February 2010.
2. *P.O. 12.3 requisitos de respuesta frente a huecos de tensión de las instalaciones eólicas*. Red Eléctrica de España, October 2006.
3. Gómez-Lázaro E, Fuentes JA, Molina-García A, Ruz F, Jimenez F. Field tests of wind turbines submitted to real voltage dips under the new Spanish grid code requirements. *Wind Energy* 2007; **10**: 483–495.
4. Jauch C, Matevosyan J, Ackermann T, Bolik S. International comparison of requirements for connection of wind turbines to power systems. *Wind Energy* 2005; **8**: 295–306.
5. Working group on grid code requirements. European grid code requirements for wind power generation. Position paper. *Tech. Rep*, European Wind Energy Association, Brussels, Belgium, February 2008.
6. Working group on grid code requirements. Harmonising europe's grid codes for the connection of wind power plants to the electricity network. *Tech. Rep*, European Wind Energy Association, Brussels, Belgium, November 2009.
7. Working group on grid code requirements. Generic grid code format for wind power plants. *Tech. Rep*, European Wind Energy Association, Brussels, Belgium, December 2009.
8. International Electrotechnical Commission. Wind turbine generator systems. Part 21. Measurement and assessment of power quality characteristics of grid connected wind turbines. *IEC 61400-21*, International Electrotechnical Commission, Geneva, Switzerland, August 2008.

Wind Energ. 2012; **15**:645–659 © 2011 John Wiley & Sons, Ltd.
DOI: 10.1002/we

9. Winter W (ed.). European wind integration study (EWIS). Towards a successful integration of large scale wind power into European electricity grids. *Final Report*, European Wind Integration Study (EWIS), Brussels, Belgium, 2010.
10. Winter W (ed.). European wind integration study (EWIS). Towards a successful integration of large scale wind power into European electricity grids. *Wind turbine model validation report*, European Wind Integration Study (EWIS), Brussels, Belgium, 2008.
11. International Electrotechnical Commission. Wind turbines. Part 27-1: electrical simulation models for wind power generation—wind turbine models (draft). *IEC 61400-27-1*, International Electrotechnical Commission, Geneva, Switzerland, 2010.
12. Ausin JC, Gevers DN, Andresen B. Fault ride-through capability test unit for wind turbines. *Wind Energy* 2008; **11**: 3–12.
13. Gómez-Lázaro E, Fuentes JA, Molina-García A, Ruz F, Jiménez F. Wind turbine modeling: comparison of advanced tools for transient analysis, *IEEE PES General Meeting*, Tampa, USA, June 2007.
14. Jiménez-Buendía F. *Modelado de los sistemas eléctricos y mecánicos de un aerogenerador doblemente alimentado: validación y aplicación a estudios eléctricos*, PhD Thesis, Univesidad politécnica de Cartagena. Escuel Técmoca Superior de Ingeniería Industrial, December 2008.
15. Gómez-Lázaro E, Fuentes JA, Molina-García A, Jiménez F. Results using wind turbine models for the certification process required by the grid codes, *International Conference on Power Systems Transients (IPST)*, Kyoto, Japan, 2009 June.
16. Martinez I, Navarro D. Gamesa DAC converter: the way for REE grid code certification. In *Power electronics and motion control conference, 2008. EPE-PEMC 2008*, 13th, 2008; 437–443.
17. Seman S, Niiranen J, Virtanen R, Matsinen JP. Low voltage ride-through analysis of 2 MW DFIG wind turbine—grid code compliance validations, *Power and Energy Society General Meeting—Conversion and Delivery of Electrical Energy in the 21st Century, 2008 IEEE*, Pittsburgh, Pennsylvania, USA, July 2008; 1–6.
18. Electromagnetic compatibility (EMC). Part 4-30: test and measurement techniques. Methods for measuring the quality of supply. *IEC 61000-4-30*, International Electrotechnical Commission, Geneva, Switzerland, August 2008.